





Article

Experimental Study on Impedance Spectrum-Based Detection of Water Holdup in Two-Phase Flow under Complex Salinity Conditions

Linfeng Cheng ^{1,2} , Shizhen Ke ^{1,2,*} , Hongwei Shi ¹ , Yuhang Zhang ¹ , Hu Luo ¹  and Hao Hu ¹ ¹ College of Geophysics, China University of Petroleum-Beijing, Beijing 102249, China² Well Logging Key Laboratory, China National Petroleum Corporation, Xi'an 710077, China

* Correspondence: wksz@cup.edu.cn

Abstract: In industrial production and water resource management involving fluid flows, two-phase flow measurement in complex environments has always been a research hotspot. In this study, a broadband detection device (40–110 MHz) suitable for two-phase flow in pipes was designed in a laboratory environment, the impedance response of two-phase flow was investigated under different salinity conditions and flow patterns, and a new impedance dispersion model suitable for two-phase flow in pipes was built. The experimental results show that the new model can better describe the rules of impedance dispersion in two-phase flow and is universally applicable, and that the equivalent solution resistance and interfacial polarization frequency have a stable functional relationship with water holdup. Based on the static experimental results, water holdup evaluation models for four flow patterns were established, and the dynamic detection results were predicted. The prediction results show that the new method proposed herein is not affected by changes in salinity and flow pattern when the flow pattern is known, and that its accuracy can meet the production requirements. This study expands the application range of traditional single-frequency conductivity detection techniques and provides a new idea for the development and improvement of systems for online detection of water holdup in two-phase flow.

Keywords: two-phase flow; impedance spectrum-based detection; water holdup; salinity; flow pattern



Citation: Cheng, L.; Ke, S.; Shi, H.; Zhang, Y.; Luo, H.; Hu, H.

Experimental Study on Impedance Spectrum-Based Detection of Water Holdup in Two-Phase Flow under Complex Salinity Conditions. *Water* **2024**, *16*, 2047. <https://doi.org/10.3390/w16142047>

Academic Editors: Helen K. French and Carlos Duque

Received: 13 June 2024

Revised: 12 July 2024

Accepted: 15 July 2024

Published: 19 July 2024



Copyright: © 2024 by the authors. Licensee MDPI, Basel, Switzerland. This article is an open access article distributed under the terms and conditions of the Creative Commons Attribution (CC BY) license (<https://creativecommons.org/licenses/by/4.0/>).

1. Introduction

Salinity is an important index for evaluating the degree of contamination of a particular body of water and determining whether the body of water can be used as a source of drinking water. In industrial processes such as oil production, accurate detection of water holdup in two-phase flow is an important basis for adjusting the injection schemes of waterflooding projects and evaluating the stage of reservoir development [1]. Therefore, acquiring accurate two-phase flow information is of great significance for the monitoring of water resources and the formulation of production and development strategies. In real production scenarios, pipes are the main carriers of two-phase flow. However, salinity and flow pattern in two-phase flow will not remain unchanged in the production process. Consequently, the measurement of two-phase flow in pipes still faces major challenges.

Existing methods for electrical detection of water holdup in two-phase flow, including the conductivity detection method and the dielectric detection method, are mainly based on the differences in conductivity and dielectric constants among oil, gas, and water. In the conductivity detection method, a large number of mineral ions are dissolved in industrial water, due to which the conductivity of industrial water is much higher than that of oil or gas. Therefore, for a two-phase mixture, water holdup information can be obtained by measuring its conductivity [2,3]. In the dielectric detection method, water is a polar molecule, and there is an additional process of molecular polarization under the action of an external electric field. At room temperature (25 °C), the relative permittivity (RP) of pure

water is 78, while the RP values of oil and gas are 2.5 and 1, respectively [4]. Water holdup detection methods based on differences in dielectric constants include the capacitance method, the radio frequency method (RFM), the microwave transmission method, and the microwave resonant cavity method [5–8]. However, the conductivity and dielectric constant of two-phase mixtures not only are related to the proportion of materials, but are also affected by flow pattern [9–11]. In order to overcome the influence of flow pattern, previous researchers have redesigned the sensor array and water holdup models. In the redesigned sensor array, multiple sensors are arranged on the pipe wall or cross-section, and information about water holdup through the whole cross-section is obtained through interpolation algorithms [12–14]. For the redesign of water holdup models, evaluation models suitable for various flow patterns have been established through experimental measurement of different flow patterns [15]. Unlike the sensor array-based detection method, the method of establishing water holdup evaluation models based on independent flow patterns does not increase the complexity of the detection instrument, and therefore it has been used as the main research approach in this study.

Existing detection methods are designed to measure either the conductivity or the dielectric constant of two-phase flow, whereas the impedance spectrum-based detection technique can obtain conductivity and dielectric constant information simultaneously. In an applied electric field, the electrical properties of a mixed medium are obviously correlated with frequency, which is known as dielectric polarization. Research data show that impedance dispersion in a mixed medium is affected by both conductivity and the dielectric constant [16,17]. On this basis, researchers established impedance dispersion models for mixed media and developed a new method for water content evaluation based on the responses of model parameters under conditions of varying water content. For example, in rock physics, the Cole-Cole model is used to evaluate water saturation in porous cores, and in electrochemistry, the Randles circuit is used to evaluate the water content of static mixed liquids. Compared with traditional single-frequency impedance detection methods, the impedance spectrum-based detection technique can obviously obtain more fluid information. In this study, an impedance spectrum-based method for detecting water holdup in two-phase flow is proposed. First, a broadband detection device for two-phase flow in pipes was built under laboratory conditions, and static and dynamic experiments were conducted under different salinity conditions and flow patterns. Then, based on the static experimental results, a new model describing impedance dispersion in two-phase flow was proposed, and a static water holdup evaluation model was established. Finally, water holdup was predicted based on the results of dynamic impedance spectrum-based detection. The prediction results show that the proposed water holdup evaluation method is not affected by flow pattern and salinity when the flow pattern is known, and it can overcome the limitations of traditional single-frequency impedance detection methods.

2. Principle

When a medium is subjected to an external electric field, polarization will occur in the medium under the action of the electric field, and the phenomenon of regular electrical dispersion will be shown macroscopically. As the frequency increases, interfacial polarization (when the frequency is <100 MHz), molecular polarization (only polar molecules, when the frequency is <10 GHz), and electronic polarization (when the frequency is >10 GHz) will occur successively in the medium [18]. It is worth noting that, when a mixed material contains an electrolyte solution, a special polarization phenomenon will occur at the interface between the electrode and the solution, which is usually called electrode polarization (<1 kHz). For this study, the frequency range is 40–110 MHz, and the object to be detected is a two-phase fluid containing water. In this setting, only interfacial polarization and electrode polarization can be observed.

2.1. Interfacial Polarization in Mixed Media

In mixed media, interfacial polarization can be divided into external interfacial polarization and internal interfacial polarization. Under the action of an external electric field, the dielectric induces a bound charge on the outer surface, and an inverse electric field is generated, which is known as external interfacial polarization. In a mixed medium, due to the difference in dielectric constants between different materials, induced charges will be produced at the interface, creating an inverse electric field. The current distribution in the interfacial polarization process satisfies Maxwell's equations in the frequency domain and can be expressed as:

$$\begin{aligned} J_o^*(\omega) &= J_c + J_d \\ &= \sigma E + j\omega \varepsilon_0 \varepsilon_r E \end{aligned} \quad (1)$$

where $J_o^*(\omega)$ is the total current density, J_c is the conduction current density, J_d is the displacement current density, σ is the conductivity, E is the electric field strength, j is the imaginary unit, $j^2 = -1$, ε_0 is the vacuum dielectric constant, whose value is 8.85×10^{-12} F/m, and ε_r is the relative dielectric constant. It can be seen from Equation (1) that the conductivity obtained by medium detection has a complex form in the frequency domain and can be expressed as:

$$\sigma^*(\omega) = \sigma + j\omega \varepsilon_0 \varepsilon_r \quad (2)$$

The detected impedance signal also has a complex form, which can be expressed as:

$$Z'(\omega) = \sigma k / (\sigma^2 + \omega^2 \varepsilon_0^2 \varepsilon_r^2) \quad (3)$$

$$Z''(\omega) = -\omega \varepsilon_0 \varepsilon_r k / (\sigma^2 + \omega^2 \varepsilon_0^2 \varepsilon_r^2) \quad (4)$$

where $Z'(\omega)$ is the real part of the impedance signal, $Z''(\omega)$ is the imaginary part of the impedance signal, and k is the ratio of the material length to the current cross-sectional area. According to Equations (3) and (4), the impedance signal contains both the conductivity and the dielectric constant of the medium. Therefore, the impedance spectrum-based detection technique can obtain more fluid information.

Equations (3) and (4) are the ideal forms of interfacial polarization in mixed materials and are difficult to use directly in actual measurement. In rock physics, the Cole-Cole model is the most widely used model because it can better describe the rules of impedance dispersion in fluid-containing porous media.

As shown in Figure 1, in the Cole-Cole model, the impedances of connected and disconnected pores are considered to be parallel. The impedance generated by the liquid phase in the connected pore space is defined as the on-solution resistance R_o , while the impedance of the disconnected pore space is defined as the polarization capacitance C_b and closed solution resistance R_b in series. Different from the ideal form of impedance dispersion, the Cole-Cole model incorporates the polarizability m (which represents the degree of polarization), the relaxation time constant τ (which describes the duration of the polarization process), and the frequency correlation index c (which describes the ideal degree of polarization capacitance) and can be expressed as [19]:

$$Z(\omega) = R_o \left\{ 1 - m \left[1 - \frac{1}{1 + (j\omega\tau)^c} \right] \right\} \quad (5)$$

$$m = \frac{R_o}{R_o + R_b} \quad (6)$$

$$\tau = C_b \left(\frac{R_o}{m} \right)^{1/c} \quad (7)$$

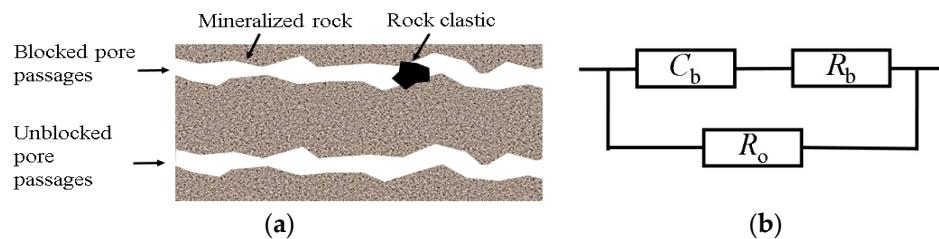


Figure 1. (a) Pore structure of porous media; (b) The Cole-Cole model.

The results show that, for porous media, the relationship of R_o and τ with water saturation satisfies a power function [17].

2.2. Electrode Polarization in Electrolyte Solutions

When measuring a mixed medium containing an electrolyte solution, the residual bound charges on the electrode surface will attract the counter-ions in the electrolyte solution, forming an electrical double layer and leading to electrode polarization. As shown in Figure 2, electrode polarization is generally described using the classical Gouy-Chapman-Stern model, which consists of an adsorption layer, a diffusion layer, and an electrically neutral solution region. In the adsorption layer, the counter-ions are closely packed under the effects of strong electrostatic interactions, resulting in a maximum concentration difference between positive and negative ions in the solution. As the electrode distance increases, the concentration difference gradually decreases and eventually reaches the electrically neutral solution region.

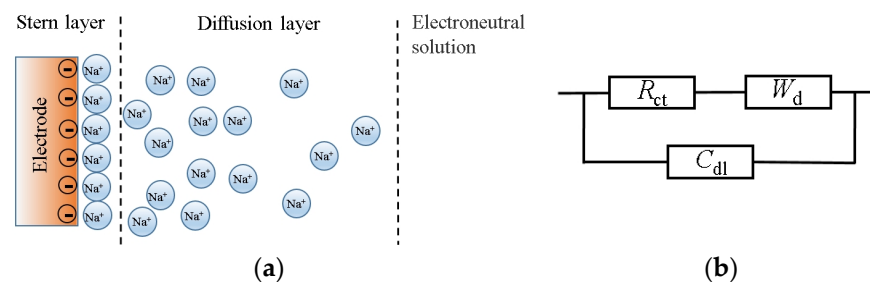


Figure 2. (a) Distribution of ions in the electrical double layer; (b) Gouy-Chapman-Stern model.

In electrochemistry, the impedance dispersion caused by electrode polarization is usually described using the classic Randles circuit. In the Randles circuit, the impedance of the electrical double layer is represented by the parallel form of the Faradaic impedance Z_F and electrical double layer capacitance C_{dl} , while Z_F is represented by the serial form of the charge transfer resistance R_{ct} and diffusion impedance W_d . Research data show that W_d cannot be expressed by a single parameter such as resistance or capacitance, but instead needs to be described by the ideal form of the Warburg impedance [20]. Therefore, the basic expression of the Randles circuit is as follows [21]:

$$Z(\omega) = \frac{R_{ct} + W_d}{1 + j\omega C_{dl}(R_{ct} + W_d)} \tag{8}$$

$$W_d = Q(j\omega)^{-0.5} \tag{9}$$

where Q is the diffusion impedance coefficient. The experimental results show that both the electrical double layer's capacitance C_{dl} and the charge transfer resistance R_{ct} have a nearly linear relationship with water content [22].

3. Experimental

In this section, static and dynamic experimental devices were designed. The reason for such design is that, under static conditions, it is relatively easy to control water holdup

and flow pattern in two-phase flow. Therefore, the model for evaluating water holdup in two-phase flow was built based on the static experimental results, and the measured results from the dynamic experiment were introduced into the model for water holdup prediction.

3.1. Experimental Setup

Figure 3a shows the static experimental device, which consists of a host computer, an impedance analyzer (Agilent4294A), a tube, and electrodes. The host computer is responsible for setting the parameters of the impedance analyzer and processing the impedance spectrum data. The working frequency of the impedance analyzer ranges from 40 Hz to 110 MHz, and the impedance analyzer can quickly measure the impedance of the two-phase mixture at 400 discrete frequency points. To facilitate observation of flow patterns and avoid signal interference, a tube made of a transparent acrylic insulation material was used. The inner diameter of the tube is 6 cm (the minimum skin depth during the experiment is 3.39 cm), and its wall thickness is 0.5 cm. There are injection holes at the top of the tube, and both ends of the tube are sealed with plugs. Stainless steel electrodes were used to avoid corrosion by the solution. In the design of electrodes, the electric field distribution in the tube also needs to be considered. In order to maintain uniform distribution of the electric field in the target tube section, the length of the target tube needs to be much smaller than the wavelength. Considering the minimum wavelength of 273 cm needed for measurement, the spacing between electrodes was set to 26 cm. As shown in Figure 3b, the dynamic experimental device comprises a water pump and an air pump to simulate the two-phase flow environment. The liquid and gas phases were fully mixed at the joint, and the mixture was routed through the target pipe section and finally returned to the water storage tank for separation and recycling.

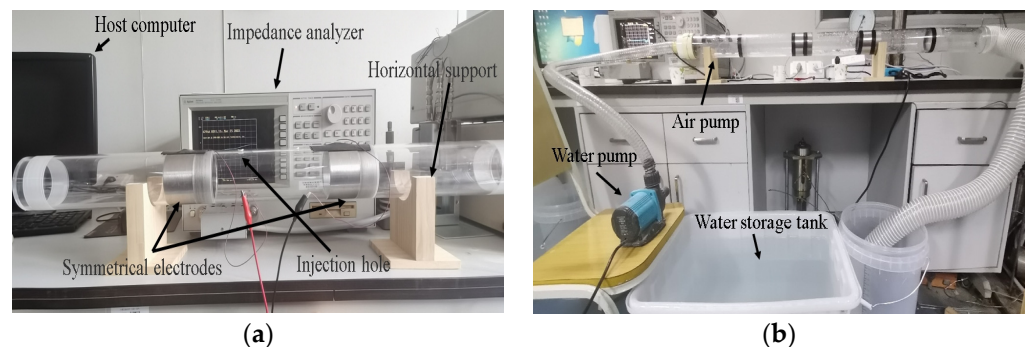


Figure 3. Design of two-phase flow detection devices. (a) Static experimental device; (b) dynamic experimental device.

3.2. Materials and Methods

The main electrolyte in groundwater is sodium chloride, and the salinity of groundwater can reach 50 g/L [23]. Therefore, for the experiment, a sodium chloride solution was used as the liquid phase, and its salinity was set to 0.5–60 g/L, including 11 concentration points. Based on the characteristics of two-phase flow in horizontal and vertical pipes, four typical flow patterns were selected for detection purposes, including laminar flow, slug flow, annular flow, and bubble flow (as shown in Figure 4). Since the conductivity and dielectric constant of gas are close to those of oil, insulating materials with low dielectric constants can be used. The insulating materials used for the experiment include glass beads and polyamide (PA6), whose dielectric constants are 2.0 and 2.2, respectively. The materials used for the different flow patterns are listed in Table 1.

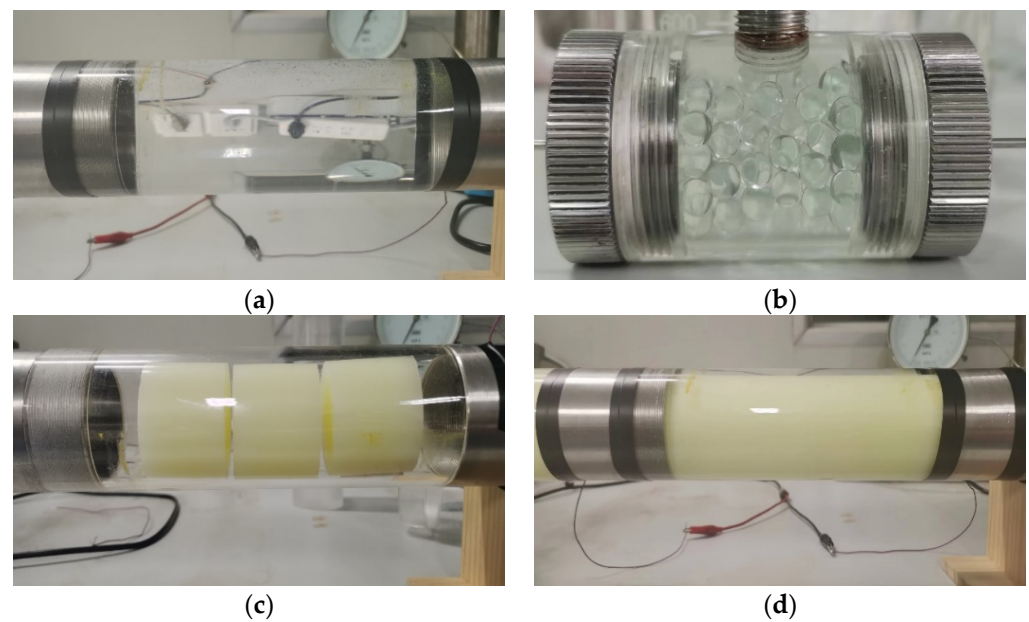


Figure 4. Flow patterns for the static experiment. (a) Laminar flow; (b) bubble flow; (c) slug flow; (d) annular flow.

Table 1. Materials used for different flow states and patterns.

Flow State	Flow Pattern	Materials
Static state	Laminar flow	Water + air
	Bubble flow	Water + glass beads
	Annular flow	Water + polyamide rod (PA6)
	Slug flow	Water + polyamide plug (PA6)
Dynamic state	Laminar flow	Water + air
	Bubble flow	Water + air
	Annular flow	Water + polyamide rod (PA6)
	Slug flow	Water + polyamide plug (PA6)

4. Results and Discussion

4.1. Impedance Dispersion Characteristics of Two-Phase Flow

Figure 5 shows the impedance dispersion curves for the four flow patterns measured under static conditions. The x -axis represents the real part of the impedance Z' , the y -axis represents the imaginary part of the impedance Z'' , the water holdup is defined as γ_w , and the salinity is defined as M_w . The experimental results show that, with an increase in frequency, Z' decreases continuously, and the amplitude of Z'' decreases in the low- and high-frequency regions and increases in the medium-frequency region. Each curve can be divided by shape into three parts, namely, the linear region, arc region, and interference region. The linear region corresponds to the process of electrode polarization in two-phase flow. As the frequency increases, the effects of electrode polarization gradually disappear, and the solution impedance is close to the pure resistance characteristic, which is defined as the solution equivalent resistance R_w , and the corresponding frequency is defined as the diffusion critical frequency f_o . The arc region corresponds to the process of interfacial polarization in two-phase flow, where the shape of the curve section is close to a semicircle. The imaginary part of the impedance Z'' has a minimum point, and the corresponding frequency is defined as the interfacial polarization frequency f_c . The interference region is a region where the interference signal generated by parasitic capacitance completely covers the real impedance signal, and the initial frequency is about 10 MHz. This part of the signal needs to be eliminated during data processing.

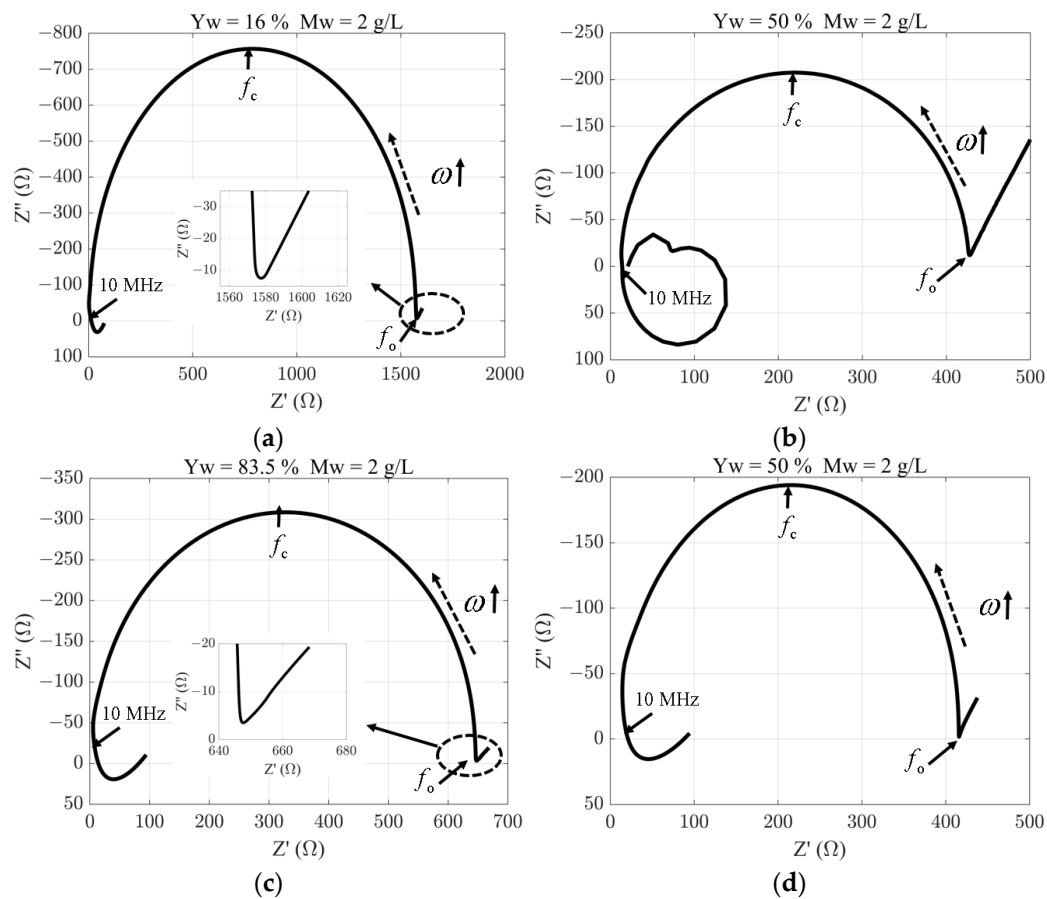


Figure 5. Impedance dispersion curve for static two-phase mixtures. (a) Annular flow; (b) bubble flow; (c) slug flow; (d) laminar flow.

Through analysis of the impedance spectra, it was found that each of the curves for the four flow patterns contained linear and arc regions, and each polarization region was independent in the frequency domain. Therefore, the equivalent circuit model for electrode polarization and interfacial polarization in series can be used to unify the expression, and the corresponding expression is as follows:

$$Z(\omega) = R_w \left\{ 1 - m \left[1 - \frac{1}{1 + (j\omega\tau)^c} \right] \right\} + \frac{R_{ct} + W_d}{1 + j\omega C_{dl}(R_{ct} + W_d)} \tag{10}$$

It is to be noted that the impedance amplitude corresponding to the highest frequency in the arc region is near 0, which means complete polarization has occurred, and the value of polarizability (m) can be set to 1. On the other hand, the relaxation curve produced by the electrical double layer at 40 Hz is almost negligible, only showing linear characteristics. This is consistent with the conclusions of a previous study [24]. Therefore, the electrode polarization process can be replaced with a non-ideal form of Warburg impedance. Equation (10) can be simplified into:

$$Z(\omega) = \frac{R_w}{1 + (j\omega\tau)^c} + Q(j\omega)^{-n} \tag{11}$$

where n is the dispersion index. Figure 6 shows the curve fitting results produced by the new model, and the rules of impedance dispersion in two-phase flow are well described in the linear and arc regions. In the actual measurement process, only complete interfacial polarization can be observed. Therefore, the relationship between model parameters and water holdup for interfacial polarization has been studied as a general topic. Previous

studies have shown that there is a stable functional relationship between the equivalent solution resistance R_w and water holdup and between the interfacial polarization frequency f_c ($f_c = 0.5\pi^{-1}\tau^{-1}$) and water holdup, while it is difficult to express the response of the frequency correlation index c to changes in water holdup using a unified functional relationship [16,22]. For this reason, only the responses of the model parameters R_w and f_c under different water holdup and salinity conditions are discussed in this paper.

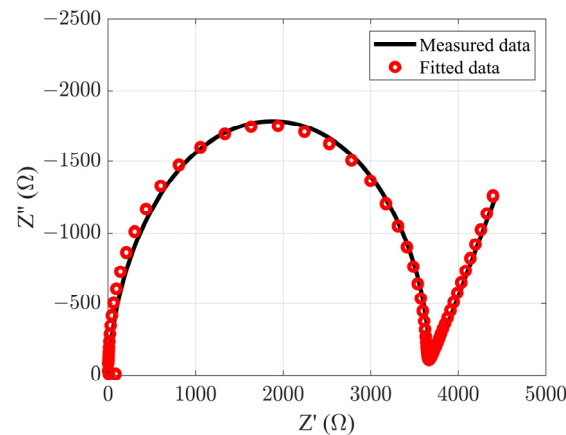


Figure 6. Prediction of impedance dispersion in two-phase flow based on the new model.

4.2. Effects of Water Holdup

As shown in Figure 7a–c, the equivalent solution impedance R_w in laminar flow, bubble flow, and annular flow is linearly related to water holdup. With the increase in water holdup, R_w decreases continuously, which is obviously related to the increase in the cross-sectional area and the radius of the diversion channel. It is worth noting that the linear slopes established under different salinity conditions are almost the same, indicating that the rate at which R_w decays with the increase in water holdup is independent of salinity. Therefore, at the linear scale, the relationship between R_w and water holdup in laminar flow, bubble flow, and annular flow satisfies a power function whose exponent is a fixed value, which can be expressed as:

$$Z_w = f(M_w)Y_w^{a_1} \quad (12)$$

where a_1 is a constant. As shown in Figure 7d, the relationship between R_w and water holdup in slug flow satisfies a linear equation, and the slope of the linear equation decreases with the increase in salinity. Therefore, it can be expressed as:

$$Z_w = f(M_w)Y_w + G(M_w) \quad (13)$$

As shown in Figure 8a–c, in double logarithmic coordinates, the interfacial polarization frequency f_c in laminar flow, bubble flow, and annular flow increases linearly with water holdup. The value of f_c is the result of the combined action of the solution capacitance and equivalent solution resistance. With the increase in water holdup, the solution capacitance increases, while the equivalent solution resistance decreases. Obviously, the effects of equivalent solution resistance on f_c are absolutely dominant. It is to be noted that the slope of the linear equation representing the relationship between f_c and water holdup at the logarithmic scale is also not affected by salinity, but, as mentioned in the impedance spectrum analysis, the signal will be disturbed and distorted when the frequency is higher than 10 MHz. Therefore, without signal distortion, the relationship between f_c and water holdup can be expressed as:

$$f_c = f(M_w)Y_w^{a_2} \quad (14)$$

where a_2 is a constant. From Figure 8d, it can be seen that the relationship between f_c and water holdup in slug flow does not satisfy a power function or a linear equation. Therefore,

it is difficult to establish a water holdup evaluation model suitable for slug flow based on such a relationship.

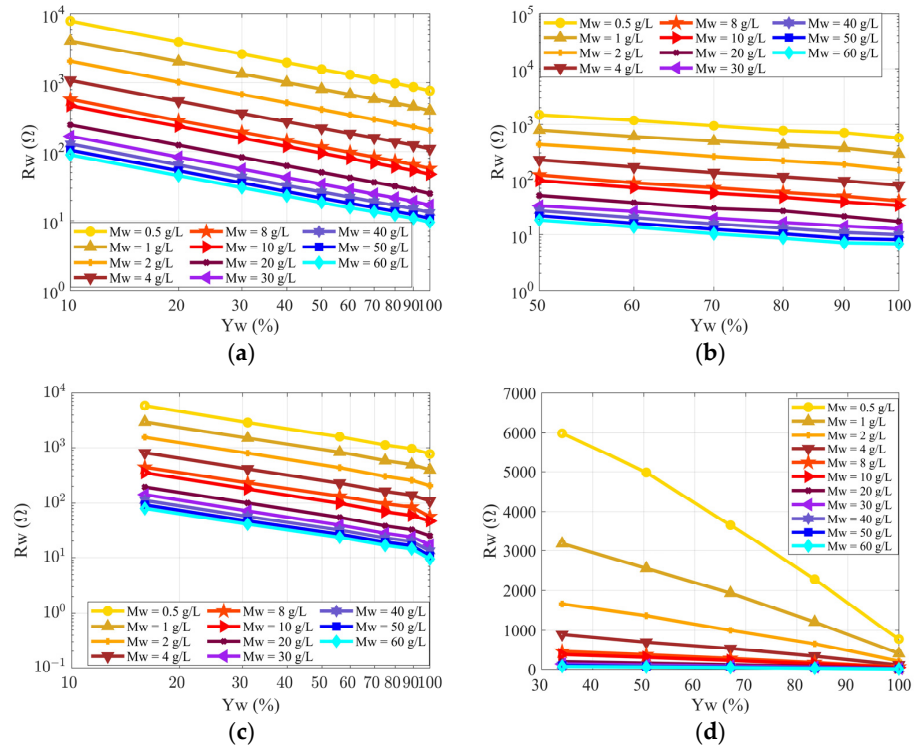


Figure 7. Relationship between equivalent solution resistance and water holdup. (a) Laminar flow; (b) bubble flow; (c) annular flow; (d) slug flow.

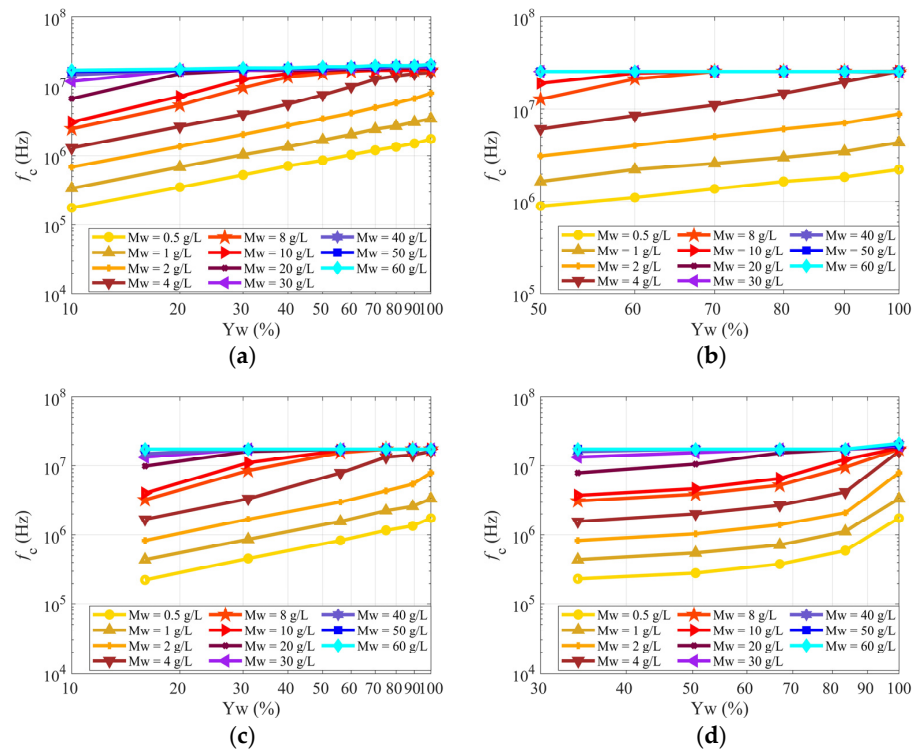


Figure 8. Relationship between interfacial polarization frequency and water holdup. (a) Laminar flow; (b) bubble flow; (c) annular flow; (d) slug flow.

4.3. Effects of Salinity

As shown in Figure 9, in double logarithmic coordinates, the equivalent solution resistance R_w under the four flow patterns decreases linearly with increasing salinity, indicating that an increase in the ion concentration of the solution improves the conductivity of the solution. It is worth noting that the slope of the linear equation representing the relationship between R_w and salinity at the double logarithmic scale is not affected by water holdup, and such a relationship can be expressed as:

$$Z_w = f(Y_w)M_w^{b_1} \tag{15}$$

where b_1 is a constant. The curves representing the relationship between the interfacial polarization frequency f_c and salinity under different flow patterns are shown in Figure 10. The experimental results show that, without signal distortion, the relationship between f_c and salinity under the four flow patterns satisfies a linear equation at the double logarithmic scale, where f_c increases with salinity. The reason is that the equivalent solution capacitance and equivalent solution impedance decrease as the concentration of conductive ions increases. Therefore, such a relationship can be expressed as:

$$f_c = f(Y_w)M_w^{b_2} \tag{16}$$

where b_2 is a constant.

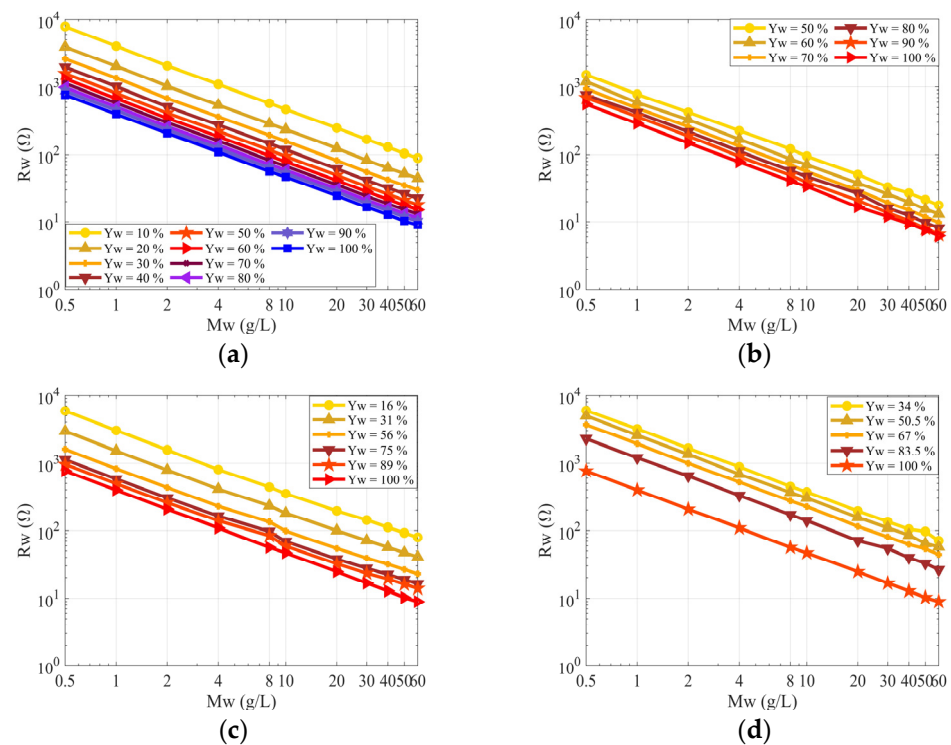


Figure 9. Relationship between equivalent solution resistance and salinity. (a) Lamina flow; (b) bubble flow; (c) annular flow; (d) slug flow.

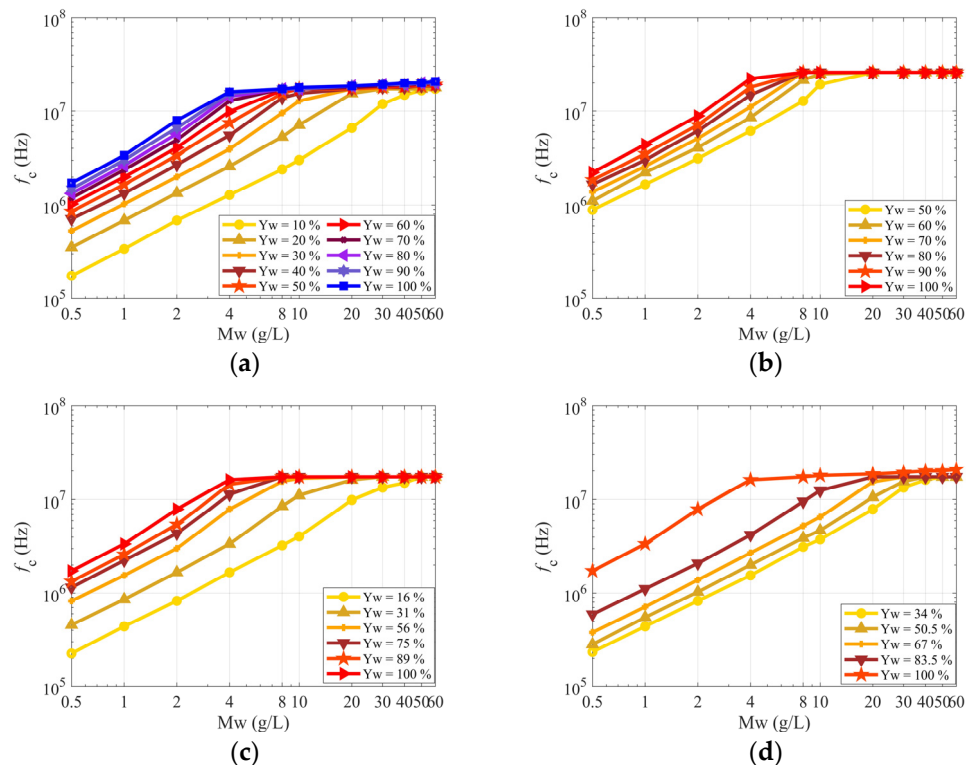


Figure 10. Relationship between interfacial polarization frequency and salinity. (a) Laminar flow; (b) bubble flow; (c) annular flow; (d) slug flow.

Considering the effects of water holdup and salinity on impedance spectra, both R_w and f_c can be represented by a functional relationship involving salinity and water holdup (as shown in Table 2). It should be noted that it is difficult to describe the relationship between f_c and water holdup in slug flow using a single function, and consequently the water holdup in slug flow cannot be quantitatively evaluated based on the value of f_c .

Table 2. Functional relationships of model parameters with salinity and water holdup.

Model Parameter	Flow Pattern	Function
$R_w(\Omega)$	Laminar flow	$4.0059 \times 10^2 Y_w^{-0.9957} M_w^{-0.9383}$
	Slug flow	$(-3.6777 Y_w + 4.0505) \times 10^3 M_w^{-0.9467}$
	Annular flow	$4.0059 \times 10^2 Y_w^{-1.0317} M_w^{-0.9359}$
	Bubble flow	$4.0059 \times 10^2 Y_w^{-1.4122} M_w^{-0.9228}$
$f_c(\text{Hz})$	Laminar flow	$4.2521 \times 10^6 Y_w^{1.0562} M_w^{1.0698}$
	Slug flow	—
	Annular flow	$4.2521 \times 10^6 Y_w^{1.3913} M_w^{1.0183}$
	Bubble flow	$4.2521 \times 10^6 Y_w^{1.1805} M_w^{0.9912}$

4.4. Dynamic Water Holdup Prediction

Compared with the measurement of water holdup in two-phase flow under static conditions, dynamic water holdup detection requires determining the effects of flow rate on impedance spectra. In previous studies, the maximum phase velocity for determining the patterns of fluid flows in pipes usually needs to be set to a value greater than 1 m/s [25]. Therefore, for the dynamic experiment, the range of flow rates was set to 0.42–1.18 m/s, including 10 measuring points, the water holdup was set to 100%, and the salinity value was set to 1 g/L. The impedance spectra at different flow rates are shown in Figure 11. The experimental results show that, under the experimental flow conditions, the electrical double layer was damaged, and the effects of electrode polarization were

further suppressed. On the other hand, the interfacial polarization processes at different flow rates were basically the same, indicating that the displacement of two-phase flow in the target pipe section during impedance measurement was almost negligible. This shows that the impedance spectrum-based technique has great potential for application in the online detection of water holdup in two-phase flow.

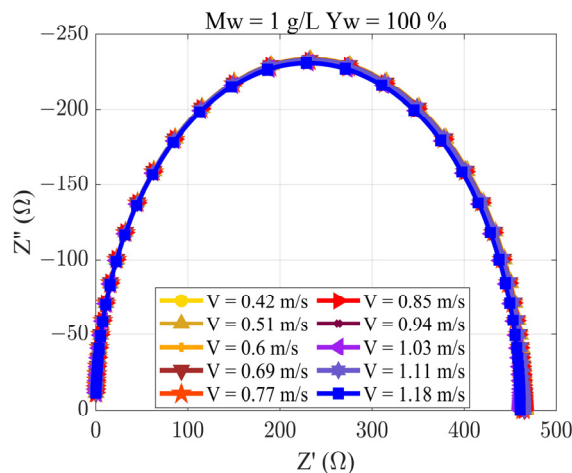


Figure 11. Impedance spectra measured at different flow rates.

In the water holdup evaluation model built based on the static experimental results, both the equivalent solution resistance R_w and the interfacial polarization frequency f_c are parameters related to interfacial polarization, and they are not affected by flow rate. Therefore, the static water holdup evaluation model can be directly used for dynamic evaluation of water holdup in two-phase flow. In order to further verify the model’s actual performance, the rates of water holdup in laminar flow ($Y_w = 100\%$), bubble flow ($Y_w = 86\%$), slug flow ($Y_w = 34\%$), and annular flow ($Y_w = 31\%$) under different salinity conditions were predicted at a flow rate of 1.18 m/s based on the measured values of the equivalent solution resistance R_w . The results are shown in Figure 12, in which the predicted data are abbreviated as “PD” and displayed by symbols, while the reference data are abbreviated as “RD” and represented by dashed lines. The experimental results show that the mean absolute errors for laminar flow, bubble flow, slug flow, and annular flow are 2.12%, 2.65%, 3.15%, and 2.78%, respectively, which do not increase with salinity.

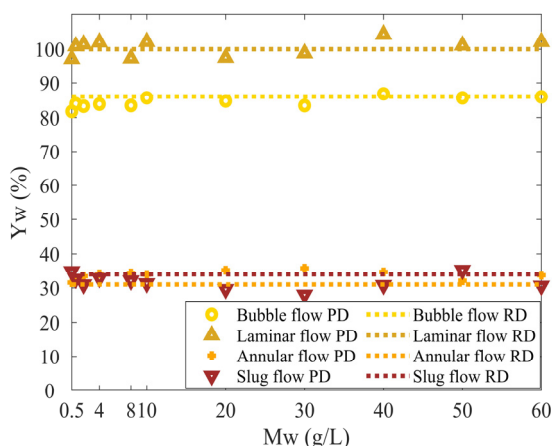


Figure 12. Values of water holdup in two-phase flow dynamically predicted based on the measured equivalent solution resistance.

5. Conclusions

A broadband detection device for two-phase flow in pipes was built, and the impedance spectra of two-phase flow under conditions of varying flow patterns, water holdups, and

salinity values were measured in the frequency range of 40–110 MHz. The experimental results show that, on impedance spectra, electrode polarization and interfacial polarization in two-phase flow are independent of each other. The spectral curve of electrode polarization is linear, while the spectral curve of interfacial polarization is circular. The rules of impedance dispersion in two-phase flow can be accurately described using a model in which electrical circuits are connected in series. The equivalent solution resistance R_w and the polarization frequency f_c can be expressed by a composite function involving salinity and water holdup, but f_c cannot be used for water holdup evaluation in slug flow and high-salinity environments. Experiments were conducted at flow rates ranging from 0.42 m/s to 1.18 m/s. The experimental results show that the interfacial polarization process was not affected by flow rate during measurement of impedance spectra. In addition, the rates of water holdup under four flow patterns were dynamically predicted under different salinity conditions. The prediction results show that the mean absolute errors are mainly distributed within the range of 2.12–3.15% and are relatively stable under different flow patterns and salinity conditions.

Author Contributions: Writing—original draft and methodology, L.C.; Conceptualization, S.K.; Validation, H.S.; Validation, Y.Z.; Investigation, H.L.; Investigation, H.H. All authors have read and agreed to the published version of the manuscript.

Funding: This research was funded by the National Natural Science Foundation of China (42074126).

Data Availability Statement: The data presented in this study are available in the article.

Conflicts of Interest: L.C. and S.K. were employed by China National Petroleum Corporation. The remaining authors declare that the research was conducted in the absence of any commercial or financial relationships that could be construed as a potential conflict of interest.

References

1. Yang, Y.; Ha, W.; Zhang, C.; Liu, M.; Zhang, X.K.; Wang, D. Measurement of high-water-content oil-water two-phase flow by electromagnetic flowmeter and differential pressure based on phase-isolation. *Flow Meas. Instrum.* **2022**, *84*, 102142. [[CrossRef](#)]
2. Wang, Y.J.; Han, J.L.; Hao, Z.Q.; Zhou, L.J.; Wang, X.J.; Shao, M.W. A new method for measuring water holdup of oil-water two-phase flow in horizontal wells. *Processes* **2022**, *10*, 848. [[CrossRef](#)]
3. Wang, D.Y.; Jin, N.D.; Zhai, L.S.; Ren, Y.Y. Salinity independent flow measurement of vertical upward gas-liquid flows in a small pipe using conductance method. *Sensors* **2020**, *20*, 5263. [[CrossRef](#)]
4. Klein, L.A.; Swift, C.T. An improved model for the dielectric constant of sea water at microwave frequencies. *IEEE Trans. Antenn. Propag.* **1977**, *25*, 104–111. [[CrossRef](#)]
5. Dai, R.S.; Jin, N.D.; Hao, Q.Y.; Ren, W.K.; Zhai, L.S. Measurement of water holdup in vertical upward oil-water two-phase flow pipes using a helical capacitance sensor. *Sensors* **2022**, *22*, 690. [[CrossRef](#)]
6. Yang, Y.; Hu, H.H.; Wang, K.; Wang, S.; Liu, M.; Zhang, C.; Wang, D. Area-alterable liquid electrode capacitance sensor for water holdup measurement in oil-water two-phase flow. *Asia Pac. J. Chem. Eng.* **2021**, *16*, e2680. [[CrossRef](#)]
7. Zuo, K.; Hong, Y.; Qi, H.T.; Li, Y.; Li, B.L. Application of microwave transmission sensors for water cut metering under varying salinity conditions: Device, algorithm and uncertainty analysis. *Sensors* **2022**, *22*, 9746. [[CrossRef](#)]
8. Xu, Y.; Zuo, R.J.; Yuan, C.; Wei, C.S.; Cao, L.F.; Sun, C.W. A water cut measurement method based on TM 010 mode microwave cavity sensor. In Proceedings of the 2022 IEEE International Instrumentation and Measurement Technology Conference (I2MTC), Ottawa, ON, Canada, 16–19 May 2022. [[CrossRef](#)]
9. Hizem, M.; Budan, H.; Deville, B.; Faivre, O.; Mosse, L.; Simon, M. Dielectric dispersion: A new wireline petrophysical measurement. In Proceedings of the SPE Annual Technical Conference and Exhibition, Denver, CO, USA, 21–24 September 2008. [[CrossRef](#)]
10. Jia, J.; Ke, S.Z.; Li, J.J.; Kang, Z.M.; Ma, X.R.; Li, M.M.; Guo, J.Y. Estimation of permeability and saturation based on imaginary component of complex resistivity spectra: A laboratory study. *Open Geosci.* **2020**, *12*, 299–306. [[CrossRef](#)]
11. Leroy, P.; Revil, A.; Kemna, A.; Cosenza, P.; Ghorbani, A. Complex conductivity of water-saturated packs of glass beads. *J. Colloid Interface Sci.* **2008**, *321*, 103–117. [[CrossRef](#)] [[PubMed](#)]
12. Wang, D.Y.; Jin, N.D.; Zhai, L.S.; Ren, Y.Y. Measurement of gas holdup in oil-gas-water flows using combined conductance sensors. *IEEE Sens. J.* **2021**, *21*, 12171–12178. [[CrossRef](#)]
13. Cherney, D.P.; Schilowitz, A.M. Detection of free water in multi-phase pipelines with AC impedance. *IEEE. Sens. J.* **2019**, *19*, 7726–7732. [[CrossRef](#)]
14. Qin, X.B.; Shen, Y.T.; Li, M.Q.; Li, M.Q.; Liu, L.; Yang, P.J.; Hu, J.C.; Ji, C.C. Visualization detection of slurry transportation pipeline based on electrical capacitance tomography in mining filling. *J. Cent. South Univ.* **2022**, *29*, 3757–3766. [[CrossRef](#)]

15. Wu, H.; Tan, C.; Dong, X.X.; Dong, F. Design of a conductance and capacitance combination sensor for water holdup measurement in oil-water two-phase flow. *Flow Meas. Instrum.* **2015**, *46*, 218–229. [[CrossRef](#)]
16. Jia, J.; Ke, S.Z.; Rezaee, R.; Li, J.J.; Wu, F. The frequency exponent of artificial sandstone's complex resistivity spectrum. *Geophys. Prospect.* **2021**, *69*, 856–871. [[CrossRef](#)]
17. Li, J.J.; Ke, S.Z.; Yin, C.F.; Kang, Z.M.; Jia, J.; Ma, X.R. A laboratory study of complex resistivity spectra for predictions of reservoir properties in clear sands and shaly sands. *J. Pet. Sci. Eng.* **2019**, *177*, 983–994. [[CrossRef](#)]
18. Garcia, A.P.; Heidari, Z. Numerical modeling of multifrequency complex dielectric permittivity dispersion of sedimentary rocks. *Geophysics* **2021**, *86*, 179–190. [[CrossRef](#)]
19. Pelton, W.H.; Ward, S.H.; Hallof, P.G.; Sill, W.R.; Nelson, P.H. Mineral discrimination and removal of inductive coupling with multifrequency IP. *Geophysics* **1978**, *43*, 588–609. [[CrossRef](#)]
20. Huang, J. Diffusion impedance of electroactive materials, electrolytic solutions and porous electrodes: Warburg impedance and beyond. *Electrochim. Acta* **2018**, *281*, 170–188. [[CrossRef](#)]
21. Randles, J.E.B. Kinetics of rapid electrode reactions. *Dis. Faraday Soc.* **1947**, *1*, 11–19. [[CrossRef](#)]
22. Qing, M.Y.; Liang, H.Q.; Zhang, J.J.; Najafabadi, H.E.; Zhan, H.L.; Leung, H. Detection mechanism of water content in oil-water emulsions by coaxial double cylinder electrodes. *IEEE Trans. Instrum. Meas.* **2020**, *70*, 1–10. [[CrossRef](#)]
23. Wu, D.Y.; Wang, C.; Yan, Y.; Shao, J.Q. Study on reducing the effect of salinity in the phase fraction measurement of oil/water two-phase flow. In Proceedings of the 2009 IEEE Instrumentation and Measurement Technology Conference, Singapore, 5–7 May 2009. [[CrossRef](#)]
24. Qing, M.Y.; Liang, H.Q.; Zhang, J.J.; Zhan, H.L. The mechanism of detecting water content in oil-water emulsions using impedance spectroscopy. *J. Pet. Sci. Eng.* **2020**, *188*, 106863. [[CrossRef](#)]
25. Trallero, J.L.; Sarica, C.; Brill, J.P. A study of oil/water flow patterns in horizontal pipes. *SPE Prod. Facil.* **1997**, *12*, 165–172. [[CrossRef](#)]

Disclaimer/Publisher's Note: The statements, opinions and data contained in all publications are solely those of the individual author(s) and contributor(s) and not of MDPI and/or the editor(s). MDPI and/or the editor(s) disclaim responsibility for any injury to people or property resulting from any ideas, methods, instructions or products referred to in the content.